

Density Induced Quantum Phase Transitions in Triplet Superconductors

R. W. Cherng

Department of Physics, Harvard University, Cambridge, MA 02138

C. A. R. Sá de Melo

School of Physics, Georgia Institute of Technology, Atlanta Georgia 30332

(Dated: April 29, 2019)

We consider the possibility of quantum phase transitions in the ground state of triplet superconductors where particle density is the tuning parameter. For definiteness, we focus on the case of one band quasi-one-dimensional triplet superconductors but many of our conclusions regarding the nature of the transition are quite general. Within the functional integral formulation, we calculate the electronic compressibility and superfluid density tensor as a function of the particle density for various triplet order parameter symmetries and find that these quantities are non-analytic when a critical value of the particle density is reached.

PACS numbers: 74.70.Kn, 73.43.Nq

Triplet superconductivity is a very rare, but very rich phenomenon in condensed matter physics. The very few confirmed examples in nature include strontium ruthenate [1] (a Ruthenium oxide) and the Bechgaard salt (TMTSF)₂PF₆ [2] (an organic molecular compound). Because the full confirmation of triplet superconductivity in solids has occurred only over the last few years, these lattice systems are not yet as fully studied theoretically and experimentally as ³He, their neutral liquid superfluid counterpart [3]. Unlike ³He, these systems are lattice charged superfluids, and their order parameters are intimately related to the lattice periodicity as in d-wave high critical temperature (T_c) superconductors [4].

It is known experimentally that electronic properties and ground states of cuprate superconductors (d-wave singlet) [4] and Strontium Ruthenate (p-wave triplet) [5] are very sensitive to chemical doping while these properties for (TMTSF)₂PF₆ (p-wave triplet) [2] are very sensitive to both external pressure and chemical doping. However, recent experiments have demonstrated that it is possible to change the carrier density electrostatically in cuprate superconductors [6] and amorphous Bismuth [7] without the introduction of additional disorder that often occurs for chemical doping. It is likely that similar electrostatic techniques will be developed for use in other superconductors like Strontium Ruthenate or (TMTSF)₂X (with X = ClO₄, PF₆). Since it may be possible in the near future to tune the carrier concentration with the use of field effect techniques, some important theoretical questions concerning these three types of systems may soon receive an experimental answer. For instance, are there quantum critical points separating magnetic and superconducting order as a function of particle density? Or, are there quantum critical points within the superconducting phase as a function of particle density? In Fig. 1 we show the zero temperature density versus interaction phase diagram indicating the existence of quantum critical lines, where the order parameter does not change symmetry but the ground

state topology changes. The elementary excitation spectrum also changes from gapless to gapped, and at finite temperatures there are three distinct regions the Fermi liquid, the pseudo-gap, and the Bose liquid regions.

In anticipation of experimental efforts, we propose to study the possible existence of topological quantum phase transitions in lattice triplet superconductors as a function of particle density. We focus on the specific case of the (TMTSF)₂X family, because they are a single-band triplet superconductors, unlike Strontium Ruthenate where three bands may be necessary to describe triplet superconductivity [5]. For this purpose, we study single band quasi-one-dimensional systems in an orthorhombic lattice with dispersion

$$\epsilon_{\mathbf{k}} = -t_x \cos(k_x a) - t_y \cos(k_y b) - t_z \cos(k_z c), \quad (1)$$

where $t_x \gg t_y \gg t_z$. We work with the Hamiltonian $H = H_{kin} + H_{int}$, where the kinetic energy part is $H_{kin} = \sum_{\mathbf{k}, \alpha} \xi_{\mathbf{k}} \psi_{\mathbf{k}, \alpha}^\dagger \psi_{\mathbf{k}, \alpha}$, with $\xi_{\mathbf{k}} = \epsilon_{\mathbf{k}} - \mu$, where μ may include the Hartree shift. The interaction part is

$$H_{int} = \frac{1}{2} \sum_{\mathbf{k}, \mathbf{k}'} \sum_{\alpha, \beta, \gamma, \delta} V_{\alpha\beta\gamma\delta}(\mathbf{k}, \mathbf{k}') b_{\alpha\beta}^\dagger(\mathbf{k}, \mathbf{q}) b_{\gamma\delta}(\mathbf{k}', \mathbf{q}) \quad (2)$$

with $b_{\alpha\beta}^\dagger(\mathbf{k}, \mathbf{q}) = \psi_{-\mathbf{k}+\mathbf{q}/2, \alpha}^\dagger \psi_{\mathbf{k}+\mathbf{q}/2, \beta}^\dagger$, where the labels $\alpha, \beta, \gamma, \delta$ are spin indices and the labels \mathbf{k}, \mathbf{k}' and \mathbf{q} represent linear momenta. We use units where $\hbar = k_B = 1$. In the case of weak spin-orbit coupling and triplet pairing, the model interaction tensor can be chosen to be

$$V_{\alpha\beta\gamma\delta}(\mathbf{k}, \mathbf{k}') = -|V_\Gamma| h_\Gamma(\mathbf{k}, \mathbf{k}') \phi_\Gamma(\mathbf{k}) \phi_\Gamma^*(\mathbf{k}') \Gamma_{\alpha\beta\gamma\delta}, \quad (3)$$

where $\Gamma_{\alpha\beta\gamma\delta} = \mathbf{v}_{\alpha\beta} \cdot \mathbf{v}_{\gamma\delta}^\dagger / 2$ with $\mathbf{v}_{\alpha\beta} = (i\sigma\sigma_y)_{\alpha\beta}$. V_Γ is a prefactor with dimensions of energy which characterizes a given symmetry. Furthermore, the term $h_\Gamma(\mathbf{k}, \mathbf{k}') \phi_\Gamma(\mathbf{k}) \phi_\Gamma^*(\mathbf{k}')$ contains the momentum and symmetry dependence of the interaction of the irreducible representation Γ with basis function $\phi_\Gamma(\mathbf{k})$ and $\phi_\Gamma^*(\mathbf{k}')$ representative of the orthorhombic group (D_{2h}).

We write down the partition function [8] $Z = \int \mathcal{D}[\psi^\dagger, \psi] \exp[-S]$ with the action $S = \int_0^\beta d\tau \left[\sum_{\mathbf{k}, \alpha} \psi_{\mathbf{k}}^\dagger(\tau) (\partial_\tau) \psi_{\mathbf{k}}(\tau) + H(\psi^\dagger, \psi) \right]$. For simplicity, we take $h_\Gamma(\mathbf{k}, \mathbf{k}') = 1$. We introduce the vector order parameter for triplet superconductivity through the Hubbard-Stratanovich transformation and integrate out the fermions to obtain the effective action

$$S_{\text{eff}} = Q_G + \int_0^\beta d\tau \sum_{\mathbf{k}\alpha} \frac{\xi_{\mathbf{k}}}{2} - \beta^{-1} \text{Tr} \ln \left[\frac{\beta \mathbf{M}}{2} \right], \quad (4)$$

where $Q_G = \int_0^\beta d\tau \sum_{\mathbf{q}, i} \mathcal{D}_i^\dagger(\mathbf{q}, \tau) \mathcal{D}_i(\mathbf{q}, \tau) / |V_\Gamma|$ and \mathbf{M} is the matrix

$$\mathbf{M} = \begin{pmatrix} [\partial_\tau + \xi_{\mathbf{k}}] \delta_{\mathbf{k}_1 \mathbf{k}_2} \delta_{\alpha\beta} & \mathbf{A}(\mathbf{k}_1, \mathbf{k}_2, \tau) \\ \mathbf{A}^\dagger(\mathbf{k}_1, \mathbf{k}_2, \tau) & [\partial_\tau - \xi_{\mathbf{k}}] \delta_{\mathbf{k}_1 \mathbf{k}_2} \delta_{\alpha\beta} \end{pmatrix},$$

where $\mathbf{A} = -\sum_i \phi_\Gamma(\frac{\mathbf{k}_1 - \mathbf{k}_2}{2}) \mathcal{D}_i(\mathbf{k}_1 + \mathbf{k}_2, \tau) \mathbf{v}_{\alpha\beta, i}$. At the saddle point, $\mathcal{D}_i(\mathbf{k}_1 + \mathbf{k}_2, \tau)$ is taken to be τ independent, and to have total Fermion center of mass momentum $\mathbf{k}_1 + \mathbf{k}_2 = 0$. Thus, $\mathcal{D}_i(\mathbf{k}_1 + \mathbf{k}_2, \tau) = \eta_i \Delta_\Gamma \delta_{\mathbf{k}_1 + \mathbf{k}_2, 0} + \delta \mathcal{D}_i(\mathbf{k}_1 + \mathbf{k}_2, \tau)$.

The order parameter equation is obtained from the stationary condition $\delta S_{\text{eff}}^{(0)} / \delta \mathcal{D}_i^\dagger = 0$, where $S_{\text{eff}}^{(0)}$ is the saddle point action

$$1 = \sum_{\mathbf{k}} |V_\Gamma| |\phi_\Gamma(\mathbf{k})|^2 \tanh(\beta E_{\mathbf{k}}/2) / 2E_{\mathbf{k}}, \quad (5)$$

where $E_{\mathbf{k}} = \sqrt{\xi_{\mathbf{k}}^2 + |\Delta_\Gamma|^2 |\phi_\Gamma(\mathbf{k})|^2}$, corresponds to the quasiparticle excitation energy. The number equation is obtained from $N = -\partial \Omega / \partial \mu$, where $\beta \Omega = -\ln Z$ is the thermodynamic potential,

$$N = N_0 + N_{\text{fluct}}, \quad (6)$$

where $N_0 = \sum_{\mathbf{k}} n_{\mathbf{k}}$, and $n_{\mathbf{k}} = [1 - \xi_{\mathbf{k}} \tanh(\beta E_{\mathbf{k}}/2) / E_{\mathbf{k}}]$ is the momentum distribution. The additional term $N_{\text{fluct}} = -\partial \Omega_{\text{fluct}} / \partial \mu$, where Ω_{fluct} are Gaussian fluctuations to saddle point Ω_0 . These two equations must be solved self-consistently, and quite generally they are correct even in the strong coupling (or low density) regime provided that $T \ll T_c$ [8], where $N_{\text{fluct}} \sim T^4$ for all couplings [9].

The saddle point vector $\mathcal{D}_i^{(0)} = \eta_i \Delta_\Gamma$ is related to the standard \mathbf{d} -vector via the relation $d_i(\mathbf{k}) = \sum_{\mathbf{k}'} \mathcal{D}_i^{(0)} \phi_\Gamma(\mathbf{k})$. In the D_{2h} point group all representations are one dimensional and non-degenerate [10], which means that the \mathbf{d} -vector in momentum space for unitary triplet states in the weak spin-orbit coupling limit is characterized by one of the four states: (1) ${}^3A_{1u}(a)$, with $\mathbf{d}(\mathbf{k}) = \hat{\eta} \Delta_{f_{xyz}} XYZ$ (“ f_{xyz} ” state); (2) ${}^3B_{1u}(a)$, with $\mathbf{d}(\mathbf{k}) = \hat{\eta} \Delta_{p_z} Z$ (“ p_z ” state); (3) ${}^3B_{2u}(a)$, with $\mathbf{d}(\mathbf{k}) = \hat{\eta} \Delta_{p_y} Y$ (“ p_y ” state); (4) ${}^3B_{3u}(a)$, with $\mathbf{d}(\mathbf{k}) = \hat{\eta} \Delta_{p_x} X$ (“ p_x ” state). Since, the Fermi surface can touch the Brillouin zone boundaries the functions X , Y , and Z need to be periodic and can be chosen

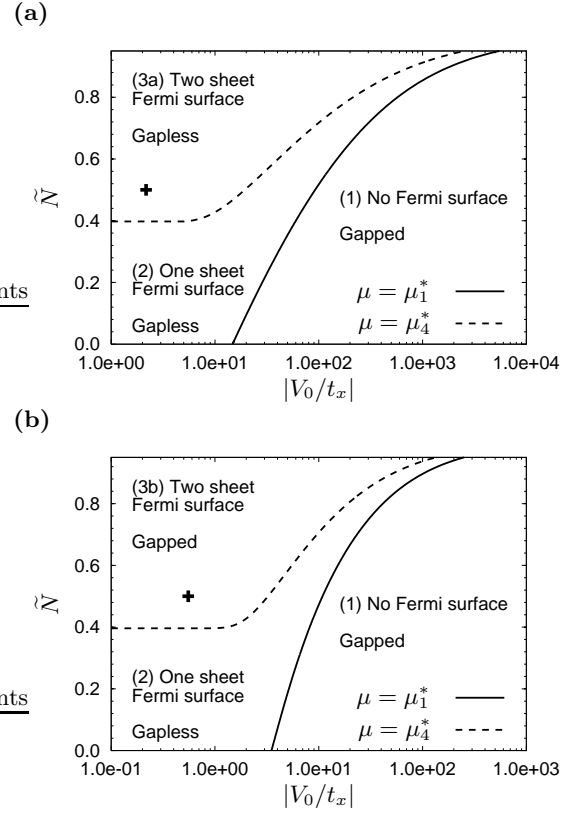


FIG. 1: Phase diagrams for (a) f_{xyz} (b) p_x symmetries based on Fermi surface connectivity and excitation spectrum. The phase diagrams are symmetric (not shown) around half-filling ($\tilde{N} = 1$) due to particle-hole symmetry. The small cross indicates the parameters compatible to the known triplet superconductor (TMTSF) $_2$ PF $_6$ $\tilde{N} = 0.5$ and $V_{p_x}/t_x = 0.5531$ for p_x , $\tilde{N} = 0.5$ and $V_{f_{xyz}}/t_x = 2.1685$.

to be $X = \sin(k_x a)$, $Y = \sin(k_y b)$, and $Z = \sin(k_z c)$. The unit vector $\hat{\eta}$ defines the direction of $\mathbf{d}(\mathbf{k})$. From here on we scale all energies by t_x . The parameters used are $t_x = 1.0000$, $t_y = 0.2144$ and $t_z = 0.0083$. It will be easier to discuss the properties of the Fermi surface and quasiparticle excitation spectrum by considering the chemical potential μ instead of the filling factor \tilde{N} . Consider the “normal state” Fermi surface defined in the first Brillouin zone (BZ) by $\xi_{\mathbf{k}} = 0$, keeping in mind the periodicity in k -space. Let us define the following characteristic values $\mu_1^* \equiv t_x + t_y + t_z$, $\mu_2^* \equiv t_x + t_y - t_z$, $\mu_3^* \equiv t_x - t_y + t_z$, $\mu_4^* \equiv t_x - t_y - t_z$. For $\mu < \mu_1^*$ the chemical potential is below the bottom of the band and there is no Fermi surface. For $\mu_1^* < \mu < \mu_2^*$ the Fermi surface consists of one connected sheet contained entirely in the first BZ and is topologically equivalent to a sphere of genus zero. For $\mu_2^* < \mu < \mu_3^*$, the Fermi surface is one connected sheet touching the edges of the BZ on the planes $k_z = \pm\pi$ equivalent to a torus of genus one. For $\mu_3^* < \mu < \mu_4^*$, the Fermi surface is one connected sheet touching the edges of the BZ on the planes $k_z = \pm\pi$

and $k_y = \pm\pi$ equivalent to a torus of genus two. Lastly for $\mu_4^* < \mu$, the Fermi surface consists of two disconnected sheets each of which touch the BZ boundary and is equivalent to two disconnected tori each of genus one.

For the superconducting state, the intersection of the Fermi surface and order parameter nodes constitute the loci of gapless quasiparticle excitations. For the p_i symmetry (where i is x , y , or z) the order parameter nodes are on the planes $k_i = 0, \pm\pi$. For the f_{xyz} symmetry, the order parameter nodes are on the union of the planes $k_i = 0, \pm\pi$, where i is x , y , and z . For all symmetries, the quasiparticle excitations are fully gapped for $\mu < \mu_1^*$ since there is no Fermi surface. For $\mu_1^* < \mu < \mu_4^*$, the order parameter nodes for all symmetries intersect the Fermi surface and hence quasiparticle excitations are gapless. For $\mu_4^* < \mu$ the Fermi surface splits into two sheets that separate along k_x so that the p_x nodes no longer intersect the Fermi surface opening a gap in the quasiparticle excitation spectrum. However, the f_{xyz} , p_z , and p_y nodes still intersect the Fermi surface so quasiparticle excitations remain gapless.

We plot representative phase diagrams for the f_{xyz} and p_x symmetries in Fig. 1. From the discussion above, the p_y and p_z phase diagrams are qualitatively similar to the f_{xyz} phase diagrams. There are three distinct phases characterized by Fermi surface connectivity and quasiparticle excitation spectrum: (1) no Fermi surface and fully gapped $E(\mathbf{k})$ for all symmetries ($\mu < \mu_1^*$), (2) one sheet Fermi surface and gapless for all symmetries ($\mu_1^* < \mu < \mu_4^*$), (3a) two sheet Fermi surface and gapless for f_{xyz} , p_z , p_y ($\mu_4^* < \mu$) (3b) two sheet Fermi surface and fully gapped for p_x ($\mu_4^* < \mu$). In addition, the (2) phase splits into three regions using the finer classification of Fermi surface topological genus: (2i) genus zero ($\mu_1^* < \mu < \mu_2^*$), (2ii) genus one ($\mu_2^* < \mu < \mu_3^*$), (2iii) genus two ($\mu_3^* < \mu < \mu_4^*$). There are several qualitative features of interest in the phase diagrams. For a fixed density and all symmetries, the chemical potential does not go below the bottom of the band ($\mu < \mu_1^*$) until a critical coupling is reached. This critical coupling is $V_{f_{xyz}}/t_x = 14.8021$, $V_{p_z}/t_x = 1.8150$, $V_{p_y}/t_x = 2.3952$, $V_{p_x}/t_x = 3.5052$ for $\tilde{N} = 0$. In addition, consider the approach to the strict one-dimensional limit ($t_y, t_z \rightarrow 0$). If $t_z \rightarrow 0$, the μ_2^* (μ_3^*) boundary merges with μ_1^* (μ_4^*) leaving only the (2ii) region. If in addition $t_y \rightarrow 0$, the μ_1^* boundary merges with μ_2^* producing only one boundary between the (1) and (3) phases.

We now turn our attention to thermodynamic quantities that provide signatures of the topological changes discussed above. In the following calculations we fix the interaction strength to be $V_{f_{xyz}}/t_x = 91.7202$, $V_{p_z}/t_x = 11.8747$, $V_{p_y}/t_x = 11.7781$, $V_{p_x}/t_x = 10.8297$, which forces $\mu = \mu_1^*$ at $\tilde{N} = 0.5$. In contrast, $\mu = \mu_4^*$ at $\tilde{N} = 0.706$, $\tilde{N} = 0.674$, $\tilde{N} = 0.672$, $\tilde{N} = 0.719$ for the f_{xyz} , p_z , p_y , p_x symmetries, respectively. The $T = 0$

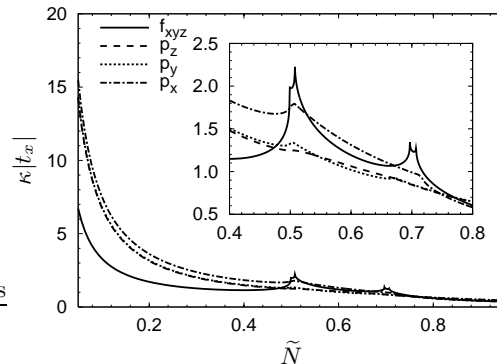


FIG. 2: Filling factor (\tilde{N}) dependence of the dimensionless electronic compressibility $\kappa|t_x|$. The inset shows the region $\tilde{N} = 0.4 - 0.8$.

electronic compressibility $\kappa = N^{-2}(\partial N/\partial \mu)_{T,V}$ is

$$\kappa = \frac{2}{N^2} \sum_{\mathbf{k}} \left[\frac{1}{2E_{\mathbf{k}}} \left(1 - \frac{\xi_{\mathbf{k}}^2}{E_{\mathbf{k}}^2} \right) \right]. \quad (7)$$

which we plot in Fig. 2. Although the compressibility does not formally diverge, there are clear anomalies (non-analyticities) when the Fermi surface topology and quasiparticle excitation spectrum change. As \tilde{N} increases, μ increases and crosses the boundaries μ_j^* where the first derivative of κ decreases discontinuously. Within the p -symmetries, the magnitude of this jump is largest for p_x . The f_{xyz} symmetry, with the presence of double or even triple nodes compared to the single nodes for the p symmetries, has the largest jumps in the derivative of κ clearly identified as the four cusps in Fig. 2. These non-analyticities in κ at $T = 0$ are indicative of a quantum phase transition. At finite temperatures the cusps in κ are smeared-out, but clear peaks are still present so long as one remains in the quantum critical region. The measurement of the electronic compressibility may be achieved in a field effect geometry [6, 7] through the relation

$$\kappa = VC_d/Q^2, \quad (8)$$

where $C_d = [\partial Q/\partial V_e]_{T,V}$ is the differential capacitance, V_e is the applied voltage, Q is the absolute value of the total charge of carriers, and V is the sample volume.

Next, we analyse the effect of phase fluctuations given by the action

$$\Delta S = \frac{1}{8} \sum_{\mathbf{q}, \omega_n} [[A(\omega_n)^2 + \rho_{ij} q_i q_j] \phi(\mathbf{q}) \phi(-\mathbf{q})], \quad (9)$$

where $A = N^2 \kappa/V$ is proportional to κ and

$$\rho_{ij} = \frac{1}{V} \sum_{\mathbf{k}} [n_{\mathbf{k}} \partial_i \partial_j \xi_{\mathbf{k}}], \quad (10)$$

is the superfluid density. Here, $n_{\mathbf{k}}$ is the momentum distribution. In Fig. 3 we show the \tilde{N} dependence of

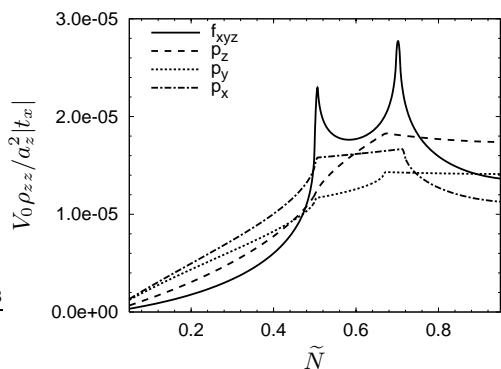


FIG. 3: Filling factor (\tilde{N}) dependence of the zz component of the dimensionless superfluid density tensor $V_0 \rho_{zz}/a_z^2 |t_x|$ for various symmetries. V_0 (a_z) is the unit cell volume (length).

the zz component of ρ_{ij} . In the case of the D_{2h} group only diagonal components ρ_{ii} exist, but they are highly anisotropic due to the quasi-one-dimensionality of $\xi_{\mathbf{k}}$.

From Eq. 10 it is clear that the zero-temperature superfluid density is the curvature of the dispersion weighted by the momentum distribution. We find the xx component is a monotonically increasing function of \tilde{N} which is best understood as a consequence of quasi-one-dimensionality. Neglecting the curvature of the Fermi surface due to finite t_x , t_y , as \tilde{N} increases, the Fermi surface encloses a monotonically increasing pocket of k -space around $k_x = 0$. In addition, below half filling the curvature of $\xi_{\mathbf{k}}$ is of the same sign in this regime so there is little cancellation between different regions of k -space. We find ρ_{yy} is also smooth but peaks in the region bounded by $\tilde{N} \approx 0.5 - 0.8$ corresponding to $\mu \approx \mu_1^* - \mu_4^*$. No longer neglecting the curvature of the Fermi surface due to finite t_y , we see that for $\tilde{N} \approx 0.5 - 0.8$, the Fermi surface encloses an increasing pocket of k -space around $k_y = 0$ up to the edge of the BZ. Since the curvature of $\xi_{\mathbf{k}}$ changes sign at $k_y = \pi/2$, cancellations between different regions of k -space eventually occur. The zz component is the most interesting as it exhibits clear anomalies such as those seen in κ . The Fermi surface varies rapidly along the k_z direction as a function of \tilde{N} so that no simple analysis in terms of contributing regions of k -space is possible. It appears that the ρ_{zz} is a more direct probe of the anomalies seen in κ with clear kinks as a function of \tilde{N} . These non-analyticities again indicate the existence of a quantum phase transition as μ is tuned below the bottom of the band.

Lastly, it is easy to extract from ΔS the phase-only collective mode frequencies via the substitution $i\omega_n \rightarrow \omega + i\delta$. In this case $\omega(\mathbf{q}) = \sqrt{(c_x^2 q_x^2 + c_y^2 q_y^2 + c_z^2 q_z^2)}$, where $c_x^2 = \rho_{xx}/A$, $c_y^2 = \rho_{yy}/A$, and $c_z^2 = \rho_{zz}/A$. These collective mode frequencies, also show similar anomalies to those of κ and ρ_{ij} , and can be used to characterize the quantum phase transition as well [9]. Notice that

$\omega(\mathbf{q})$ is anisotropic reflecting the orthorhombic structure. For instance, $\omega(q_x, 0, 0) = c_x q_x$, $\omega(0, q_y, 0) = c_y q_y$, and $\omega(0, 0, q_z) = c_z q_z$, where c_i is the speed of sound along the i -th direction. However, these modes may be plasmonized in a charged superfluid.

In summary, we studied possible quantum phase transitions in triplet superconductors, as the density of carriers is changed, provided that the Cooper pairing interaction is sufficiently attractive. For organic quasi-one-dimensional conductors (Bechgaard salts) only one quantum phase transition may be accessible experimentally as the interaction strength is too weak to cross both phase boundaries as a functions of filling factor (See Fig. 1). However, these quantum phase transitions may be possible in optical lattices where the attractive interaction may be changed via Feshbach resonances, thus allowing the system to cross the phase boundary separating the weak and strong interaction regimes [11]. In order to identify these quantum phase transitions (QPT) where the symmetry of the order parameter does not change, we classified Fermi surface topologies and excitation spectrum properties as a function of filling factor for weak spin-orbit coupling symmetries f_{xyz} , p_x , p_y and p_z . We then related non-analyticities in the electronic compressibility and superfluid density to quantum phase transitions between various phases. We would like to thank NSF (Grant No. DMR-0304380) and NDSEG for support.

-
- [1] Y. Maeno *et al.*, Nature, **372**, 532 (1994).
 - [2] I. J. Lee *et al.* Phys. Rev. Lett., **88**, 017004 (2002).
 - [3] A. J. Leggett, Rev. Mod. Phys., **47**, 331 (1975).
 - [4] Elbio Dagotto, Rev. Mod. Phys., **66**:763, 1994.
 - [5] A. P. Mackenzie and Y. Maeno, Rev. Mod. Phys., **75**:657, 2003.
 - [6] C. H. Ahn, J. M. Triscone, and J. Mannhart. Nature, **424**, 1015 (2003).
 - [7] K. A. Parendo *et al.*, Phys. Rev. Lett., **94**, 197004 (2005).
 - [8] J. R. Engelbrecht, M. Randeria, and C. A. R. Sá de Melo. Phys. Rev. B, **55**, 15153 (1997).
 - [9] For low densities and strong interactions, Landau damping is absent at zero temperature for all symmetries since the elementary excitation spectrum is gapped. At low densities and weak interactions, the gap closes and there is Landau damping at low energies because Cooper pairs near the nodal regions can decay into the two-particle continuum. However, the system is still underdamped and the low temperature behavior of N_{fluct} is controlled by T^4 . At higher densities and weak interactions, the gap reopens in the p_x symmetry and Landau damping is absent while p_y , p_z , and f_{xyz} symmetries remain gapless but underdamped.
 - [10] R. D. Duncan, C. D. Vaccarella, and C. A. R. Sá de Melo, Phys. Rev. B, **64**, 172503 (2001).
 - [11] K. Gunter *et al.*, cond-mat/0507632.